

DOI: 10.1002/cssc.201((will be completed by the editorial staff))

# A hybrid supercapacitor based on porous carbon and MOF MIL-100(Fe)

Nicolo` Campagnol<sup>[a]</sup>, Ricardo Romero Vara<sup>[ab]</sup>, Willem Deleu<sup>[c]</sup>, Linda Stappers<sup>[a]</sup>, Koen Binnemans<sup>[d]</sup>, Dirk E. De Vos<sup>[c]</sup> and Jan Fransaer<sup>\*[a]</sup>

Hybrid supercapacitor electrodes based on carbon nanotubes, carbon black and a Metal Organic Framework (MOF) with iron(III) coordination centres (MIL-100(Fe), MIL-88(Fe) and MIL-53(Fe)) have been prepared and tested with several aqueous electrolytes. A correlation between hydrated ion size and the electric response of the electrodes was found, which sheds light on how these materials

work as energy storage devices. MIL-100(Fe) shows the most promising results, and the capacitance obtained with the samples with the solutions used is higher than that of a mix of carbon and nanotubes in the same solution. Unfortunately shortcomings due to reductive dissolution still hamper the cyclability of the electrodes.

## Introduction

The interest in energy storage devices has boomed in the last years due to several new needs: use of intermittent energy generated by green sources, longer autonomy and miniaturization of portable devices, and the search for competitive cost and performance for hybrid and electric cars. Supercapacitors (SCs) are an evolution of classic capacitors and one of the most promising technologies for the future energy storage. Similarly to their predecessors, they are based on electrostatic principles but, thanks to the introduction of an electrolyte, they possess a higher capacitance given by the double layer at the electrodes (electric double layer supercapacitors) and/or by Faradaic reactions (pseudocapacitors).<sup>[1]</sup> The introduction of Faradaic reactions makes the difference with batteries not as sharp anymore as for classic capacitors. As a matter of fact, the energy and power density of SCs are now in between those of batteries and capacitors.<sup>[2]</sup>

Various nomenclatures have been proposed for SCs but none is yet commonly accepted.<sup>[1, 2]</sup> For this work we use the definition of hybrid capacitor as a SC based on two mechanisms: pseudocapacitance given by Faradaic reactions on the surface, and supercapacitance given by the electric double layer.<sup>[3]</sup>

The current pursuit of new functional materials led to the discovery of ultraporous compounds called Metal Organic Frameworks (MOFs). MOFs are formed by metal centres (metal ions or clusters of metal and oxygen) connected by bridges of organic molecules. MOFs are formed by metal centres (metal ions or clusters of metal and oxygen) connected by bridges of organic molecules. The obtained structure is light and hollow leading to very high specific surface areas, e.g. ~6000 m<sup>2</sup>g<sup>-1</sup> in the case of the Cr-BDC (BDC = 1,4-benzenedicarboxylic acid) MIL-101(Cr).<sup>[4]</sup> Every MOF has a characteristic structure with mesopores and nanopores of different dimensions. These cavities of the structure are only accessible via windows whose dimensions are also determined by the MOF structure, normally spanning from few nm or less than one.

Even though the lack of conductivity of these materials is still an unsolved problem,<sup>[5]</sup> the high specific surface area of MOFs has inspired various authors to investigate their electrochemistry, in particular in applications like SCs.<sup>[6]</sup> Other possibilities in the field of energy storage have been proposed, and MOFs have been tested as separators,<sup>[7]</sup> positive<sup>[8]</sup> and negative<sup>[9]</sup> electrodes for Li-ion batteries, and as separators for fuel cells.<sup>[10]</sup> Another interesting application in this field has been proposed by the group of Tarascon<sup>[11]</sup> who explored the behaviour of Cr-BTC MIL-100(Cr) (BTC = benzenetricarboxylic acid) as cathode for Li-S batteries.

Yeon Lee et al. studied a Co-BDC MOF obtaining very high capacitance and outstanding cycle life; only 1.5% of the 205 F/g was lost after 1000 cycles in alkaline media.<sup>[12]</sup> Simultaneously was reported the synthesis and study of a Zn-BDC MOF where the metal centres are partially substituted by cobalt.<sup>[13]</sup> This MOF, in which zinc is partially substituted by cobalt, is reported to have a good cycle life but a very low capacitance (0.5 F/g referred to total mass of the electrode), mostly given by the 10 wt% of carbon added to make the samples.

No investigation of iron-based crystalline MOFs has been reported up to now, but the electrochemical activity of a commercial non-crystalline compound based on iron and 1,3,5-benzenetricarboxylic acid,<sup>[17]</sup> the same components of MIL-100(Fe), has been reported by Babu et al.<sup>[18]</sup>

[a] MEng. N. Campagnol, MEng.R. Romero-Vara, Dr. L. Stappers, Prof. Dr. J. Fransaer

Department of Metallurgy and Materials Engineering (MTM), KU Leuven, Kasteelpark Arenberg 44, B-3001 Leuven, Belgium  
Jan.Fansaer@mtm.kuleuven.be

[b] M.Eng. R. Romero-Vara

Department of Materials Engineering, Escuela Técnica Superior de Ingenieros Industriales. Universidad Politécnica de Madrid.  
José Gutiérrez Abascal, 2. 28006 – Madrid, Spain

[c] MEng W. Deleu, Prof. Dr. D. E. De Vos

Centre for Surface Chemistry and Catalysis (COK), KU Leuven, Kasteelpark Arenberg 23, B-3001 Leuven, Belgium

[d] Prof. Dr. K. Binnemans

Department of Chemistry, KU Leuven, Celestijnenlaan 200F P.O. Box 2404, B-3001 Leuven, Belgium

Supporting information for this article is available on the WWW under <http://dx.doi.org/10.1002/cssc.20xxxxxx>. ((Please delete if not appropriate))

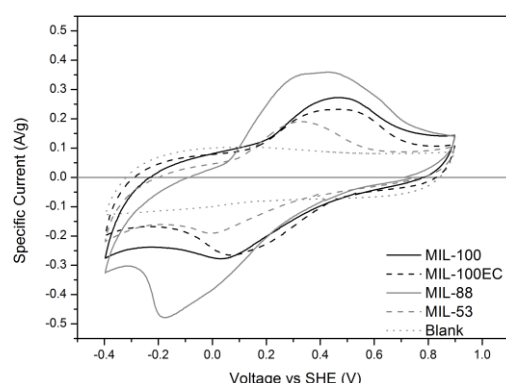


**Figure 1.** Cyclic voltammograms in 0.1 M  $\text{Cs}_2\text{SO}_4$  solution at 5 mV/s scan rate of MOF50A (MIL-100), MOF50B (MIL-100 EC), MOF50C (MIL-88), MOF50D (MIL-53) and blank.

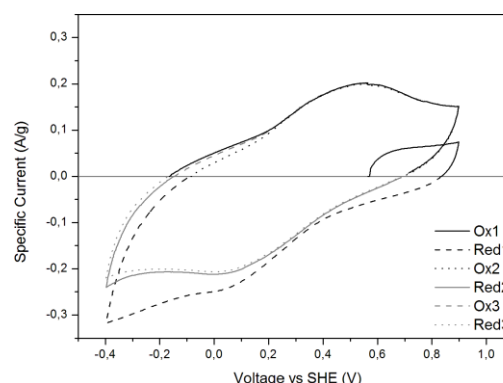


**Figure 2** Cyclic voltammogram in aqueous 0.1 M  $\text{Na}_2\text{SO}_4$  solution at a scan rate of 5 mV/s of MOF50A. The scan starts from the anodic branch and no oxidation peak can be observed since the iron centres are in the  $\text{Fe}^{3+}$  state (Ox1). After the first reduction branch (Red1) is completed, the centres of the material are in the  $\text{Fe}^{2+}$  state and can be afterwards oxidized back to  $\text{Fe}^{3+}$  (Ox2).

**Table 1.** Comparison between MOF50 and a blank sample (70% NT, 20% CB and 10% PTFE) in an aqueous 0.1 M  $\text{Cs}_2\text{SO}_4$  solution. The first samples exhibit two redox peaks due to the pseudocapacitance while the last has only EDLC.

Sample	MOF	$E_{1/2}$ (V vs SHE)	Pores diameter in nm and type	Brea- thing	$C_{cv}$ (F/g)
MOF50A	MIL-100	0.22	2.9-2.5 (3D) <sup>[14]</sup>	N	62
MOF50B	MIL-100 <sup>[a]</sup>	0.26	2.9-2.5 (3D) <sup>[14]</sup>	N	50
MOF50C	MIL-88	0.10	2.3 (3D) - 3.8 (1D) <sup>[15]</sup>	Y	84
MOF50D	MIL-53	0.16	0.86 (1D) <sup>[16]</sup>	Y	40
Blank	-	-	-	N	26

[a] Electrochemically synthesised

Cyclic voltammetry (CV) on a small amount of Basolite® F300 particles, immobilized on a platinum or carbon electrode, shows a redox reaction at +0.24 V vs. SHE. CVs run in acidic media show an influence of the pH on the current density but not in the peak separation. After 20 cycles, no difference was found in the electrochemical response: both peak intensity and separation remained the same as in the first cycle.

In this work we demonstrate how the electrochemical response of crystalline MOFs is influenced by both the pore dimensions and by the redox reaction of the iron centres. The hybrid composite electrodes we used are prepared by mixing a MOF (MIL-53, MIL-88, or MIL-100) with carbon nanotubes and carbon black. The kinetics of the electrodes is investigated with CV, studying the influence of thickness and scan rate. We explore the effect of different cations in solution in relation to the dimension of the pores. Different solvents, anions and cation concentrations are also investigated. Finally we report the effect of multiple cycles (up to 200) on the electrochemical capacitance of the material

for a possible application as SC electrode comparing the results with those of a blank sample cycled in the same conditions.

## Results and Discussion

MIL-100(Fe) powders were characterized by XRD and scanning electron microscopy (SEM). SEM pictures of the single constituents and of a MOF50A sample show that the different components (MOF, carbon nanotube, carbon black and PTFE particles) are well mixed, see Figure S1. Also the other synthesized MOF powders were systematically analysed by XRD to prove their high degree of crystallinity, the patterns are reported in S2.

Figure 1 shows the cyclic voltammograms measured with MOF50A, MOF50B, MOF50C, MOF50D, and a blank sample in 0.1 M  $\text{Cs}_2\text{SO}_4$  aqueous solution. The response of the blank is merely an Electric Double Layer Capacitance (EDLC), while the MOF50 samples show a mix of EDLC given by the carbon material and the pseudocapacitance due to the  $\text{Fe}^{3+}/\text{Fe}^{2+}$  redox couple of the MOF. For each material, the average of the anodic and cathodic peak positions (redox potential) is found at different potentials, see Table 1. MOF50 samples based on MIL-100 (both synthesized electrochemically and solvothermally) have a redox potential at *circa* +0.22-0.26 V vs. SHE. This is very similar to the +0.24 V vs. SHE recorded with a commercial material based on the same constituents as MIL-100(Fe), namely iron and BTC, in an acidic environment.<sup>[18]</sup> As already reported with other coordination compounds,<sup>[21,22]</sup> the values are very different from the standard  $\text{Fe}^{3+}/\text{Fe}^{2+}$  reduction potential at 25 °C (+0.771 V vs SHE), but in contrast with other reported compounds, the peak separation is somehow wider. Based on elemental and Mössbauer analyses, the iron centres of the MIL-100(Fe) structure are reported to be in the  $\text{Fe}^{3+}$  state.<sup>[23, 24]</sup> The CV shown in Figure 2 is in accordance with this: when the CV is started from the anodic branch (Ox1), no oxidation peak can be detected since the iron centres are

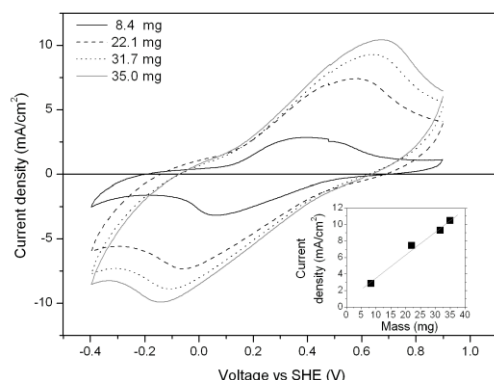


**Figure 3.** Cyclic voltammograms in aqueous 0.1 M  $\text{Cs}_2\text{SO}_4$  solution (pH 7) at scan rate of 5 mV/s of MOF50A samples with different masses (8.4, 22.1, 31.7 and 35.0 mg). In the inset is reported the linear relation between the maximum current density and the mass of the electrodes

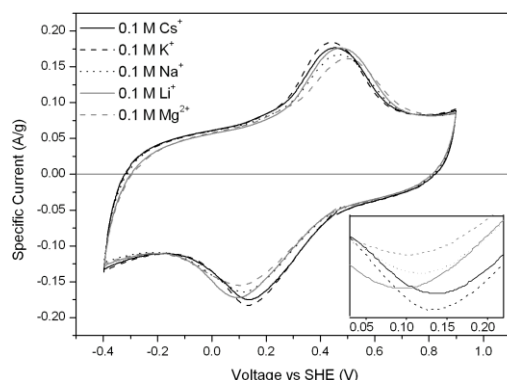


**Figure 4.** Cyclic voltammograms in aqueous 0.1 M  $\text{Cs}_2\text{SO}_4$  solution at scan rates of 1, 5, 10, 50, 75 and 100 mV/s of MOF50, scaled to show the specific capacitance ( $C_v$ ) variation. In the inset the relation between capacitance, specific current, and scan rate

already in the oxidized  $\text{Fe}^{3+}$  state. The oxidation of  $\text{Fe}^{2+}$  to  $\text{Fe}^{3+}$  ( $\text{Ox}_2$ ) only occurs after the metal centres are reduced to the  $\text{Fe}^{2+}$  state during the cathodic part of the cycles ( $\text{Red}_1$ -2). The amount of coordination centres oxidized or reduced at each cycle can be estimated comparing the areas below the curves recorded with MOF50 and with a blank sample. As example can be taken the reduction parts of the CVs of MOF50A and of the blank sample reported in Figure 1. The difference in the calculated area of the two curves can be divided by the scan rate and multiplied by the amount of MOF in the sample resulting in a charge of 0.07 C. Assuming that each electron oxidizes from  $\text{Fe}^{2+}$  to  $\text{Fe}^{3+}$  one atom of iron, this charge can be divided by the elementary charge and leads to  $4.12 \times 10^{17}$  iron centres addressed during one half of a CV cycle. Considering that in MIL-100(Fe) for each mole of compound there are 3 moles of iron, and that the molar mass of dehydrated MIL-100(Fe) is 659 g/mol,<sup>[24]</sup> in 5 mg of this MOF there are  $2.28 \times 10^{-5}$  moles of iron, or  $1.37 \times 10^{19}$  iron centres. From this calculation we can conclude that 3% of the iron

centres are oxidized during the first cycle, or 9% of the trimmers assuming the oxidation of one iron centre per trimer. The result corresponds to one quarter of the maximum amount reachable thermally degassing the material at 260 °C.<sup>[23]</sup> This lower percentage is partially due to the low intermixing of the conductive and non-conductive phases, and mostly to the low conductivity of the MOF itself which does not allow electrons to travel through the structure when an iron centre is reduced/oxidized.

An important parameter in the study of electrodes for supercapacitors is the sample thickness.<sup>[20]</sup> Also with our samples, we observed that the electrochemical activity is proportional to the mass, and therefore the thickness, of the composite layers (Figure 3). Moreover, the cyclic voltammograms show that the anodic and cathodic peaks shift to higher and lower potential respectively as the electrode thickness increases. This shift is due to the slowing down of the overall reaction kinetics since the increase in the thickness of the electro-active material decreases the accessibility of the electrolyte, and therefore the positive alkali ions, into the electrode material. A linear model fits extremely well with the distribution of the data ( $R^2 = 0.99$ ), as can be seen in the inset, and shows that, even if the kinetics are reduced, the same percentage of material is active regardless of the sample dimensions. In order to study the kinetics of the system, CVs with aqueous 0.1 M  $\text{Cs}_2\text{SO}_4$  solution at different scan rates have been carried out with MOF50A samples, see Figure 4. To have a better understanding of the results, the CV have been plotted showing the maximum specific capacitance obtainable from the samples. In the SI the same data are plotted versus specific current.

Visible redox peaks have been obtained at 1 mV/s, 5 mV/s and 10 mV/s, while at 50 mV/s, 75 mV/s and 100 mV/s no observable electrochemical activity was found. Scan rates faster than 50 mV/s do not give the time to the ions of the solution to penetrate the lattice resulting in a redox reaction detectable with a redox peak, and therefore the pseudocapacitance at these scan rates is lost. The decrease of obtained capacitance with the increasing of the scan rate is exponential, see inset of Figure 4, and a similar trend was observed with different Co MOF.<sup>[27]</sup>

CVs have been run with three MOFs: MIL-100(Fe) synthesized electrochemically and solvothermally, MIL-53 and MIL-88, see Table 1. All three MOFs are based on iron centres and benzene-carboxylic acids, and the main differences in their structure are the arrangement of the Fe ions and the type of pores: MIL-100 has 3D pores accessible via windows of different dimensions, MIL-53 has only straight channels, and MIL-88 features both types of pores. MIL-53, and partially MIL-88, have a flexible structure, while MIL-100 does not change its structure upon adsorption and desorption. Moreover MIL-100 is based on trimesic acid (benzenetricarboxylic acid) and has therefore three connections per linker molecule and not two as is the case of terephthalic acid (benzenedicarboxylic acid). In Figure 1 is reported a comparison of the CV obtained with the MOFs tested. Almost no difference can be seen in the shape of the CV curves measured with MIL-100 synthesized with different techniques, but the resulting specific currents of the samples synthesized electrochemically are apparently lower, possibly due to a non-perfect structure obtainable with this technique.<sup>[19]</sup>

**Table 2.** Capacitance and redox potential ( $E_{1/2}$ ) measured with MOF50 samples in different electrolytes, the Shannon ionic diameters and the diameters of the hydrated ions.<sup>25</sup>

Electrolyte (0.1 M)	pH	$E_{1/2}$ (V vs SHE)	$C_{cv}$ (F/g)	Ion	Ionic diameter (nm) <sup>25</sup>	Hydrated diameter (nm) <sup>26</sup>	Desolvation energy (kJ/mol) <sup>26</sup>
Cs <sub>2</sub> SO <sub>4</sub>	6.2	0.30	34	Cs <sup>+</sup>	0.38	0.66	- 250
K <sub>2</sub> SO <sub>4</sub>	5.6	0.29	36	K <sup>+</sup>	0.30	0.66	- 295
Na <sub>2</sub> SO <sub>4</sub>	5.9	0.34	34	Na <sup>+</sup>	0.20	0.72	- 365
Li <sub>2</sub> SO <sub>4</sub>	5.5	0.29	34	Li <sup>+</sup>	0.12	0.76	- 475
MgSO <sub>4</sub>	5.7	0.31	32	Mg <sup>2+</sup>	0.14	0.86	- 1830

As can be observed in Figure 1, MIL-88 has the highest initial current density, but the stability of this MOF is much lower than that of MIL-100, and after 50 CVs the whole signal is given by the carbon material, see S6.

MIL-53 is apparently the worst performing of the batch since its signal is lower and it is lost after about 100 cycles, see S8. Nevertheless it is interesting to observe how the breathing structure responds differently in comparison to the more fixed ones of MIL-100 and MIL-88. In the first five cycles the reduction peaks, connected with the insertion of alkaline ions from the solution, grow to higher values (see S8), and only after the fifth cycle the material starts to visibly suffer of reductive dissolution.

As reported in literature,<sup>[28, 29]</sup> the size and charge of the cations in solution are important parameters to determine the electrochemical response of porous materials. CVs measured at 5 mV/s show the different response of MOF50 samples in solutions containing ions of the first and second group of the periodic table (Figure 5 for MOF50A, S7 for MIL50C and S9 for MIL50D). The results are summarized in Table 2 and show how the peaks proximity and also partially the capacitance ( $C_{cv}$ ) scale with the inverse of the hydrated size of the cation in solution, and Cs has therefore the highest value. This is a remarkable finding since it gives crucial information on the mechanism of interaction between MOF pores and the ions of an electrolyte. Desolvation of the ions in solution is not needed to enter the 2.9 nm diameter mesopore of MIL-100(Fe), since its 0.86 nm diameter windows 14 are larger than all the solvated ions reported in Table 2. The smaller mesopores are 2.5 nm in diameter, and to enter these cavities desolvation is necessary for all the ions in the list since the 0.55 nm diameter windows are smaller than the hydrated shell of all the ions. If the hydration shell were stripped from the cations in solution, one would expect to record the highest current density, and therefore capacitance, using ions with the smallest ionic diameters, like Li<sup>+</sup> or Mg<sup>2+</sup>. Notwithstanding, even though it has been reported that this desolvation takes place in carbon electrodes<sup>[29, 30]</sup> and in narrow channels,<sup>[31]</sup> in our case Cs<sup>+</sup> and K<sup>+</sup> show the highest signals. Tests with Mg<sup>2+</sup> ions give results slightly off from the alkali series, but similar to those recorded with Li<sup>+</sup>, as expected from the similar hydrated diameters. Thanks to this data we can discard the desolvation energy to be the sorting factor since the value for Mg<sup>2+</sup>, reported in Table 2, is much higher than that of Li<sup>+</sup> or another

alkali ion. It can be concluded that ions with small hydrated diameters have a higher penetration in MOF MIL-100(Fe) lattice. A similar result was reported for another coordinated compound based on iron centres, Prussian blue, with which a similar selectivity was observed.<sup>[32]</sup> Changing the solvent from water to ethanol confirms our observation: no Faradaic activity is observed in a 0.2 M solution of KOAc in ethanol, while in an aqueous solution with the same concentration of salt, the resulting activity is very similar to that observed with K<sub>2</sub>SO<sub>4</sub> (S5). The result is again in agreement with the literature and might explain why the material used by Diaz<sup>[13]</sup> did not live up to the expectations: in their work they employed the traditionally used large tetrabutylammonium ion (from the TBAPF<sub>6</sub> salt) in a non-aqueous solvent (acetonitrile), seeing no redox activity, while in this work and in those of Lee et al.<sup>[12, 27]</sup> aqueous solvents with small ions are used. We can speculate that the different behaviour with the ions in solution observed with MIL-100 in comparison to carbon materials is due to two main factors: the hydrophilicity of this MOF and lack of conductivity of its structure. Carbon materials are generally hydrophobic and conductive; hence the solvent molecules, whether coming from the solution or from the solvation shell of the cations dissolved, are generally kept outside its structure.

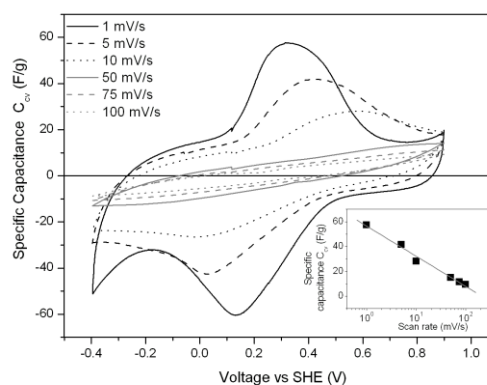


**Figure 5.** Cyclic voltammograms of MOF50 in aqueous 0.1 M Li<sub>2</sub>SO<sub>4</sub>, Na<sub>2</sub>SO<sub>4</sub>, K<sub>2</sub>SO<sub>4</sub>, Cs<sub>2</sub>SO<sub>4</sub>, and MgSO<sub>4</sub> solution at 5 mV/s scan rate.



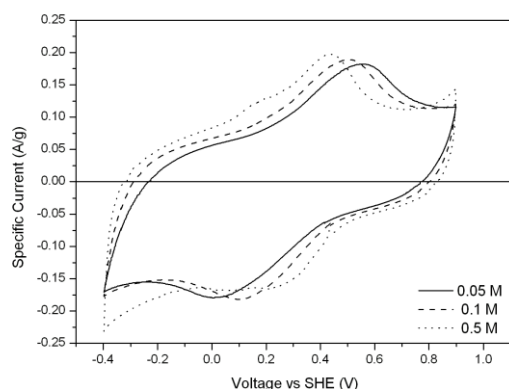


**Figure 6.** Cyclic voltammograms of MOF50A in 0.05 M, 0.1 M, and 0.5 M  $K_2SO_4$  solutions at 5 mV/s.

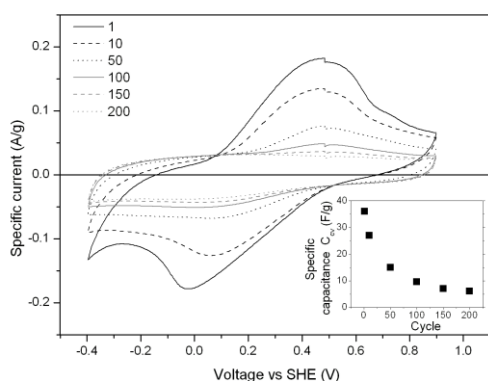


**Figure 7.** Cyclic voltammograms in 0.1 M  $Cs_2SO_4$  solution at 5 mV/s of MOF50 after 1, 10, 50, 100, 150, and 200 cycles and of the background material.

Thanks to the conductivity of most carbon structures, their channel walls can accumulate charges to form a double layer with the water molecules stripped from the ions. On the other hand, MIL-100(Fe) is hydrophilic and the non-conductive structure of its channels apparently does not allow the creation of an electric double layer. The ions therefore enter the structure in a solvated state where they compensate the change in valence of the iron centres.

A similar trend can be observed also with MIL-88 (S6). Probably due to the breathing of the framework, samples containing MIL-53 give biased results with different solutions. As can be observed in the CVs taken during cycling, the redox peaks shift at lower or higher potential at each cycle, without a predictable scheme, and therefore changing the solution it is not possible to understand whether the shift is due to the cycling or to the different ion present. The effect of the ion size in MOF50 samples is not influenced by the presence of the carbon material since, as reported in the S10, the response of blank samples in different solution is the same.

The effect of the anion has also been studied using three solutions with constant cation concentration: 0.1 M  $K_2SO_4$ ,



**Figure 8.** Stability tests of MIL-100 in different solutions. From left: 0.2 M KOAc in ethanol, demineralised water, 0.1 M  $K_2SO_4$ , 0.2 M LiOH, 0.2 M KOH, 0.2 M KCl, and 0.2 M KOAc, all in water.

0.2 M KOAc and 0.2 M  $KNO_3$ , and is reported in S5. The anion influences the anodic peak height and peak position. A shift to higher potentials can be observed in the cathodic peak using the sulphate solution. This occurrence is probably due to the different concentration (0.1 M instead of 0.2 M) used with this anion. In fact we report that ion concentration in solution is very important for the electrochemical response of the samples. Figure 6 shows three CVs taken with a MOF50A sample in 0.05 M, 0.1 M, and 0.5 M  $K_2SO_4$  solutions. The redox potential and the peak intensity are barely influenced by the different solutions, while the separation of the peaks decreases with the increase in cation concentration. This phenomenon can be the base for a possible application of MOFs in electrochemical sensors.

Electrochemical tests have been run to investigate the cyclability of the composite material. The MOF50 samples were cycled at 5 mV/s between -0.4 and 0.9 V vs SHE for 200 cycles in aqueous 0.1 M  $Cs_2SO_4$  solution at pH 7. As can be seen from Figure 7 with MOF50A (and in S6 for MOF50C and S8 for MOF50D), the electrodes gradually lose part of their electrochemical properties. The change from  $Fe^{2+}$  to  $Fe^{3+}$  damages the structure of the MOF apparently irreversibly, a process called reductive dissolution. The dissolution is not due to the contact with the solution since MIL-100(Fe) is very stable in pure water<sup>[33]</sup> and in all the electrolytes used in this work.

Figure 8 shows an experiment on the stability of this MOF: MIL-100(Fe) powder was immersed for seven days in 0.2 M KOAc dissolved in ethanol, demineralised water, and 0.1 M  $K_2SO_4$ , 0.2 M LiOH, 0.2 M KOH, 0.2 M KCl, and 0.2 M KOAc aqueous solutions. From an optical analysis and from the XRD patterns (S11) it is clear that this MOF is stable in all solutions except the strongly alkaline ones.

These results forced us to use different electrolytes than that proposed by Lee et al.<sup>[12, 27]</sup> who worked with Co-based MOFs in 0.5 M LiOH aqueous solutions. These electrolytes are surely

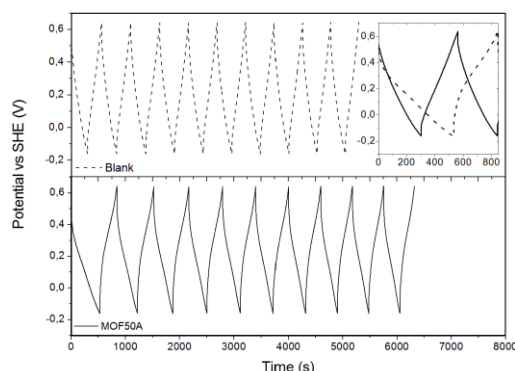


**Figure 9.** Galvanostatic charge-discharge cycling at 0.1 A/g in 0.1 M K<sub>2</sub>SO<sub>4</sub> solution of a blank sample and MOF50A. Due to the redox reaction the curves do not look straight like those taken with the blank material, typical of EDLC capacitors. Unfortunately reductive dissolution takes place and a reduction of the charge storable can be seen at each cycle.

less performing but also less harmful for humans and the environment.

In order to study the reductive dissolution in our experiments, an 0.1 M K<sub>2</sub>SO<sub>4</sub> solution was analysed before and after cycling a MOF50A sample 100 times in it. After the experiment, the liquid, originally clear and transparent, was tinted yellow and an orange precipitate (probably an iron sulphate due to its low solubility) was observed on the bottom of the cell.

The precipitate was dissolved decreasing the pH to 2 with nitric acid, and the iron concentrations of both solutions were measured with Inductively Coupled Plasma mass spectrometry (ICP). In the starting solution the concentration of iron is 0.031±0.007 ppm, while after 100 cycles the iron concentration increased to 7.3±0.080 ppm. Considering this concentration it is possible to calculate the amount of iron dissolved in the 80 mL cell, 1.044×10<sup>-5</sup> mol, *circa* half of what is expected if all the MOF of the electrode would dissolve in solution.

When all the MOF material is consumed by reductive dissolution, the response of the sample is given by the background material. The shape of MOF50A sample's curve after 200 cycles is very similar to that of the blank sample reported in Figure 1, and the obtained current density is about half. The other two MOFs tested show even lower resistance to cycling and after 50-100 cycles no more redox reactions occur. The ratio in current density is in good agreement with what is expected if half of the mass of MOF50 is not active anymore since it is half of what has been measured with blank samples. In S3 are reported the XRD patterns of MOF50 samples before and after cycling and it can be observed how the signal of MIL-100 is completely lost after 200 cycles and only the big peak due to the carbon compounds is left.

Thanks to the presence of the background material and the relatively large amount of MOF in the samples, it is possible to observe the reductive destruction/disintegration of this phase and explain the loss of performance with cycling. The carbon part of the electrodes is resistant to cycling and its response does not change after one or 200 cycles, see SI.

Figure 9 reports the galvanostatic charge-discharge cycling measured in a three electrodes set-up at 0.1 A/g in K<sub>2</sub>SO<sub>4</sub> solution of a blank sample and MOF50A. As expected,<sup>20,34,35</sup> the curves recorded with MOF50 are not straight due to

the redox reaction occurring at the metal centres of the MOF. Even though the capacity measured with MOF50A is higher than the blank, the discharge time decreases with the cycles due to reductive dissolution, as seen also in the CVs (Figure 6). The specific capacitance (C) with the sulphate solution is quite low, only 39 F/g during the first discharge, but it is still higher than the capacitance obtained with the carbon material alone (32 F/g) in the same conditions. This is again an evidence that in aqueous media, if a better stability is the redox reaction is achieved, MOFs might improve the performance of currently used materials for supercapacitors.

## Conclusions

The main goal of the research was to investigate the electrochemical activity of some iron-based MOFs and their possible use as hybrid supercapacitor electrodes. Electrochemical activity is observed in aqueous electrolytes during cyclic voltammetry at slow scan rates, while at high it is hard to detect the redox peaks. As expected from coordinated compounds, the reduction potential of the Fe<sup>3+</sup>/Fe<sup>2+</sup> couple differs from the value of the standard one and it is different for each MOF used. The electrochemical activity of the samples made out of carbon and MOF scales with the electrode thickness and slightly with the inverse of the hydrated cation size.

It is observed that Cs<sup>+</sup> and K<sup>+</sup> show a higher penetration in MOF MIL-100(Fe) and MIL-88(Fe) lattice than lighter ions, leading to redox peaks closer to the equilibrium potential and with higher current densities.

In contrast with what has been reported for pure carbon materials, the insertion kinetics is determined by the hydrated size of the cations in solution and not by the unhydrated one, suggesting that the desolvation of the ions on the surface does not take place in our system, at least for the MOF part. We can conclude that the electrochemical response and the pseudocapacitance storable in the tested MOFs are given both by the porous morphology of the MOF and by the redox activity of the Fe centres. If a conductive MOF with redox centres could be found, the amount of metal centres reduced and oxidized would probably increase, increasing the pseudocapacitance and possibly obtaining also some electric double layer capacitance from the surface.

In view of a possible application as an energy storage device, the cyclic stability of the material should be improved. Reductive dissolution deteriorates the contribution of the MOF to the capacitance until, after maximum 200 cycles, the capacitance is determined only by the carbon material. The hybrid SC electrodes exhibit in a three electrode set-up a maximum capacitance of 39 F/g in 0.1 M K<sub>2</sub>SO<sub>4</sub> solution, *circa* 20% more than a mix of carbon black and carbon nanotubes, and the material is therefore promising for energy storage if the degradation of the MOF material during cycling can be halted.

## Experimental Section

### 2.1 Electrode preparation

Crystalline MIL-100(Fe) powder was synthesized electrochemically and solvothermally. For the solvothermal

synthesis the solution was composed of 4.8 g iron(III) nitrate ( $\text{Fe}(\text{NO}_3)_3$ , 99% purity Sigma-Aldrich, Germany), 1.64 g of 1,3,5-benzenetricarboxylic acid ( $\text{H}_3\text{BTC}$  98% Sigma-Aldrich, Germany), and 0.45 g of hydrofluoric acid (HF 48 wt%, Sigma-Aldrich, Germany) in 60 mL of demineralized water. The reactants were introduced in a pressure vessel which was heated in a microwave oven (Milestone, Italy) to 140 °C for 30 minutes. The electrochemical synthesis has been recently reported by our group<sup>19</sup> and consists in the anodic dissolution (10 mA for 30 min at 110 °C) of iron in a solution composed by 20 g/L of methyltributylammonium methyl sulphate (MTBS,  $\geq 95\%$ , Aldrich Germany) and 20 g/L of 1,3,5-benzenetricarboxylic acid ( $\text{H}_3\text{BTC}$ , 98% ABCR, Germany) in absolute ethanol (99.9%, VWR France). After both syntheses, the powder was recovered by centrifugation, washed several times with warm ethanol and dried at 70 °C overnight.

MIL-88B was synthesized in a 250 mL Schott flask containing 50 mL of *N,N*-dimethylformamide (DMF, Acros organics 99+%) Sequentially were added to the solvent: 1.66 g of terephthalic acid (Acros organics, 99+%), 4 mL of 2M NaOH solution and 2.70 g of  $\text{FeCl}_3 \cdot 6\text{H}_2\text{O}$  (Sigma Aldrich >99%). The flask was sonicated until the liquid was clear and then placed in the oven for 18 h at 100 °C. The powder was recovered by centrifugation and washed several times with warm DMF and warm ethanol, and dried at 60 °C and at 150 °C overnight.

MIL-53 was synthesized as follows: 6 g of  $\text{FeCl}_3 \cdot 6\text{H}_2\text{O}$  (Aldrich, 97%), 3.7 g of 1,4-benzenedicarboxylic acid (Aldrich, 98%), and 1.2 mL of hydrofluoric acid (Aldrich, 40% purity) were dissolved in 100 mL DMF (Aldrich 99%) and 3.2 mL of  $\text{H}_2\text{O}$  and stirred under reflux for 3 h. The obtained powder was filtered and washed several times with warm DMF and warm ethanol, and dried at 60 °C and at 150 °C overnight. X-Ray Diffraction (XRD) patterns (S2) confirm that the structures of the obtained powders are those of MIL-100, MIL-88 and MIL-53 respectively.

Composite electrodes (MOF50) were assembled on stainless steel disks (1.5 cm diameter) for the electrochemical tests. To produce these electrodes, a paste was made mixing 50 wt% of MOF, 35 wt% of carbon nanotubes (CN, Nanocyl, Belgium), 10 wt% of carbon black (CB, Degussa Evonik, Germany), and 5 wt% of polytetrafluoroethylene powder (PTFE, ICI Chemicals&Polymers, UK) in ethanol. The suspensions were ultrasonically mixed and then stirred manually until a paste was obtained. This paste was placed between a stainless steel current collector and a filter paper (Macherey-Nagel, Germany), pressed at 500 kg/cm<sup>2</sup> and dried at room temperature overnight. To evaluate the contribution of the carbon materials to the electrochemical response, composite electrodes composed of 70 wt% CN, 20 wt% CB and 10 wt% PTFE were produced similarly (blank). The MOF50 samples made with different MOFs are designated using different letters, as reported in Table 1.

## 2.2 Electrochemical tests

All samples were tested in a three electrode setup specifically designed to keep in every experiment the same distances between the electrodes. A circular platinum foil with an area of 5.5 cm<sup>2</sup>, much larger than the working electrode (1.3 cm<sup>2</sup>), was used as counter electrode, and a  $\text{Hg}/\text{Hg}_2\text{SO}_4$  with saturated  $\text{K}_2\text{SO}_4$  electrode (Schott Instruments, Germany) was used as reference electrode. Cyclic voltammetry (CV) and galvanostatic

measurements were performed with a potentiostat/galvanostat (EG&G Princeton model 273, USA).

Different aqueous electrolytes were used for the characterization of the samples, all with a cation concentration of 0.2 M. The salts used are the following:  $\text{Li}_2\text{SO}_4$  (Aldrich-Chemie),  $\text{Na}_2\text{SO}_4$  (Acros),  $\text{K}_2\text{SO}_4$  (Acros),  $\text{Cs}_2\text{SO}_4$  (Sigma-Aldrich),  $\text{MgSO}_4$  (Acros), potassium acetate (KOAc, Applychem), and  $\text{KNO}_3$  (Chemlab). For each solution, the electrochemical window was calculated based on the pH and the temperature, using the Nernst equation. In literature the specific capacitance of materials (*C*) in F/g is calculated in two ways: either from CVs as the ratio of the maximal specific current (*i*) in mA/g divided by the scan rate in mV/s ( $dU/dt$ ):  $C = i/(dU/dt)$ ; or in galvanostatic measurements with the same formula using the specific current (*i*) times the discharge/charge time in s (*dt*) divided by the potential window used.<sup>[20]</sup>

The second is the one which should be used for numerical comparison since it is the most realistic way to simulate the behaviour of the material in SCs applications. In this paper we call the first  $C_{cv}$  and the second simply *C*.

## Acknowledgements

The authors thank IWT for support in the SBO-project MOFShape. The authors are grateful to Nanocyl for providing the nanotubes necessary for the samples and in particular Carmen Tola who was the direct intermediary. The authors thank the European Commission for their support via the Erasmus program.

**Keywords:** supercapacitors • metal-organic frameworks • MIL-100 • MOF • hybrid supercapacitor

- [1] a) S. Chen, W. Xing, J. Duan, X. Huc, and S. Zhang Qiao, *J. Mater. Chem. A*, **2013**, *1*, 2941; b) M. Conte, *Fuel Cells*, **2010**, *10*(5), 806.
- [2] M. Winter and R.J. Brodd, *Chem. Rev.*, **2004**, *104*, 4245
- [3] A. K. Shukla, A. Banerjee, M. K. Ravikumar, and A. Jalajakshi *Electrochim. Acta*, 2012, **84**, 165.
- [4] S. H. Jung, J. H. Lee, J. W. Yoon, C. Serre, G. Férey, and J. S. Chang, *Adv. Mater.*, **2007**, *19*, 121.
- [5] G. Givaja, P. Amo-Ochoa, C. J. Gomez-Garcia, and F. Zamora, *Chem. Soc. Rev.*, **2012**, *41*, 115.
- [6] A. Morozan and F. Jaouen, *Energy Environ. Sci.*, **2012**, *5*, 9269.
- [7] B. M. Wiers, M.-L. Foo, N. P. Balsara and J. R. Long, *J. Am. Chem. Soc.*, **2011**, *133*, 14522.
- [8] G. Férey, F. Millange, M. Morcrette, C. Serre, M.L. Doublet, J.M. Grenèche, and J.M. Tarascon. *Angew. Chem. Int. Ed.*, **2007**, *18*, 3259.
- [9] X. Li, F. Cheng, S. Zhang and J. Chen, *J. Power Sources*, **2006**, *160*, 542.
- [10] H. Kitagawa, *Nat. Chem.*, **2009**, *1*, 689.
- [11] R. Demir-Cakan, M. Morcrette, F. Nouar, C. Davoisne, T. Devic, D. Gonbeau, R. Dominko, C. Serre, G. Férey and J.-M. Tarascon, *J. Am. Chem. Soc.*, **2011**, *133*, 16154.
- [12] D. Y. Lee, S. J. Yoon, N. K. Shrestha, S.H. Lee, H. Ahn and S. H. Han, *Micropor. Mesopor. Mater.*, **2012**, *153*, 163.
- [13] R. Diaz, M. G. Orcajo, J. A. Botas, G. Calleja, J. Palma, *Mater. Lett.* **2012**, *68*, 126.
- [14] G. Férey, C.S., C. Mellot-Draznieks, F. Millange, S. Surblé, J. Dutour, and I. Margiolaki, *Angew. Chem. Int. Ed.*, **2004**, *116*, 6456.
- [15] S. Surblé, C.S., C. Mellot-Draznieks, F. Millange and G. Férey *Chem. Comm.*, **2005**, *3*, 284.

- [16] P. Horcajada, T. Chalati, C. Serre, B. Gillet, C. Sebrie, T. Baati, J. F. Eubank, D. Heurtaux, P. Clayette, C. Kreuz, J. S. Chang, Y. Hwang, V. Marsaud, P. N. Bories, L. Cynober, S. Gil, G. Férey, P. Couvreur, R. Gref, *Nat. Mater.*, **2010**, 9, 172.
- [17] A. Dhakshinamoorthy, M. Alvaro P. Horcajada E. Gibson M. Vishnuvarthan A. Vimont J. Grenèche C. Serre M. Daturi H. Garcia 2010, *ACS Catal.*, **2010**, 2, 2060.
- [18] K. F. Babu, M. A. Kulandainathan, I. Katsounaros, L. Rassaei, A. D. Burrows, P. R. Raithby, and F. Marken, *Electrochem. Commun.*, **2010**, 12, 632.
- [19] N. Campagnol, T. Boudewijns, T. Van Assche, J. Denayer, K. Binnemans, D. E. De Vos, and J. Fransaer, *J. Mat. Chem. A*, **2013**, 1, 5827.
- [20] M. D. Stoller and R. S. Ruoff, *Energy Environ. Sci.*, **2010**, 3, 1294.
- [21] J. Ping, J. Wu, K. Fan, and Y. Ying, *Food Chem.*, **2011**, 126, 2005.
- [22] A. A. Karyakin, *Electroanal.*, **2000**, 13, 813.
- [23] J. W. Yoon, Y. K. Seo, Y. K. Hwang, J. S. Chang, H. Leclerc, S. Wuttke, P. Bazin, A. Vimont, M. Daturi, E. Bloch, P. L. Llewellyn, C. Serre, P. Horcajada, J. M. Grenche, A. E. Rodrigues, and G. Férey, *Angew. Chem. Int. Ed.*, **2010**, 49, 5949
- [24] P. Horcajada, S. Surble, C. Serre, D. Y. Hong, Y. K. Seo, J. S. Chang, J. M. Grenèche, I. Margiolakid, and G. Férey, *Chem. Commun.*, **2007**, 2820.
- [25] I. Persson, *Pure Appl. Chem.*, **2010**, 82(10), 1901
- [26] a) A.G. Volkov, S. Paula, and D.W. Deamer, *Bioelectroch. Bioener.*, **1997**, 42, 153; b) Y. Marcus, *Biophys. Chem.*, **1994**, 51, 111
- [27] D. Y. Lee, D.V. Shinde, E.K. Kim, W. Lee, I. Oh, N. K. Shrestha, J. K. Lee, S.H. Han, *Micropor. Mesopor. Mater.*, **2013**, 171, 53.
- [28] A. J. Bard and L. R. Faulkner, in *Electrochemical methods: fundamentals and applications* Ch. 13, 545 (Wiley, New York, 2000).
- [29] J. Chmiola, G. Yushin, Y. Gogotsi, C. Portet, P. Simon, and P. L. Taberna, *Science* **2006**, 313, 1760.
- [30] J. Chmiola, C. Largeot, P. L. Taberna, P. Simon, and Y. Gogotsi, *Angew. Chem. Int. Ed.*, **2008**, 47, 3392.
- [31] R. M. Lynden-Bell and J. C. Rasaiah, *J. Chem. Phys.*, **1996**, 105, 9266.
- [32] M. Hartmann and E.W. Grabner, *Anal. Chim. Acta*, **1991**, 242, 249.
- [33] P. Kűsgens, M. Rose I. Senkovska H. Frűde A. Henschel S. Siegle S. Kaskel, *Micropor. Mesopor. Mat.*, **2009**, 120, 325.
- [34] W. Chen, R. B. Rakhi, and H. N. Alshareef, *J. Mat. Chem. A*, **2013**, 1, 3315-24.
- [35] D. Liu, X. Wang, X. Wang, W. Tian, J. Liu, C. Zhi, D. He, Y. Bando, and D. Golberg, *J. Mat. Chem. A*, **2013**, 1, 1952-55.

Received: ((will be filled in by the editorial staff))

Published online: ((will be filled in by the editorial staff))



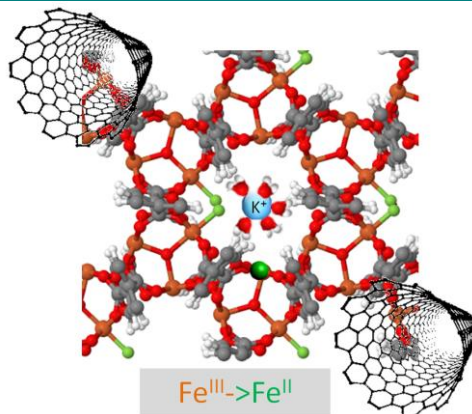
Entry for the Table of Contents (Please choose one layout)

Layout 1:

## FULL PAPER

### Metal Organic Frameworks with Carbon Nanotubes for the future energy storage

Hybrid supercapacitors electrodes based on MOFs (MIL-100, MIL-88, and MIL-53) and CNT have been tested with environmental friendly electrolytes. The energy storage mechanism followed by these materials is explored and explained, and promising results have been obtained with the



Nicolo` Campagnol, Ricardo Romero Vara, Willem Deleu, Linda Stappers, Koen Binnemans, Dirk E. De Vos and Jan Fransaer\*

Page No. – Page No.

**A hybrid supercapacitor based on porous carbon and MOF MIL-100(Fe)**